CHAPTER 4

Growth Models

Most of the progress that has been made in the study of aggregation phenomena in the last few years has derived from numerical simulations carried out on models of growth mechanisms. Dynamical features enter here due to the irreversible nature of these systems; time has a direction.

The complexity of the phenomena is reduced by supposing an elementary process to be the dominant mechanism, an assumption later confirmed. A simple model of cellular growth was proposed along these lines by Eden in 1961 to account for the tumor proliferation.

4.1 The Eden model

In its simplest version, this model constructs clusters on a lattice. As in the case of percolation, a cluster is composed of connected sites, two sites being connected if they are first neighbors. Cluster growth occurs by, at the end of each unit interval of time (taken as constant), an empty site, called a growth site, becoming occupied. In the Eden model, the growth sites, G, are those neighboring the cluster sites (i.e., the sites already occupied) (Fig. 4.1.1). The process begins with a germ (or seed, or nucleation site), which might, for example, be a line as shown in Fig. 4.1.2. Each new site occupied at time n is drawn at random from the growth sites G at time n–1.

Note that slight modifications to this site model (bond model) can easily be made, as they were to the percolation model.

When a (computer generated) Eden cluster is examined (see Fig. 4.1.3), it is found to be compact (except for a few holes close to the surface), but its surface is found to be rather tortuous.

The mass–radius relation in a d-dimensional Euclidean space takes the form

$$M \propto R^d ,$$

that is, its geometry is dense.

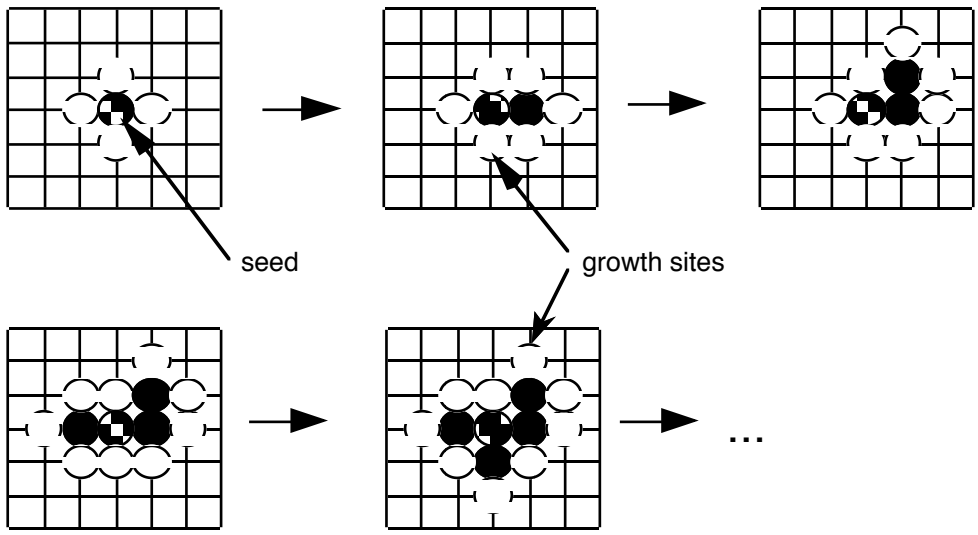

Fig. 4.1.1. Construction of an Eden cluster on a square lattice. The model simulates the proliferation of malignant cells (in black) starting from a single cell (the germ) by contamination of the closest neighbors (growth sites, in white). This contamination is assumed to occur at random within the set of growth sites.

Let us examine the surface structure in greater detail. To characterize this more easily it is helpful to choose instead other initial conditions, thereby avoiding the problems of radial geometry. The germ is taken to be the line $h = 0$ and periodic boundary conditions are chosen (column $x = L+1$ is identified with column $x = 0$). Growth can, of course, take place in higher ($d > 2$) dimensions.

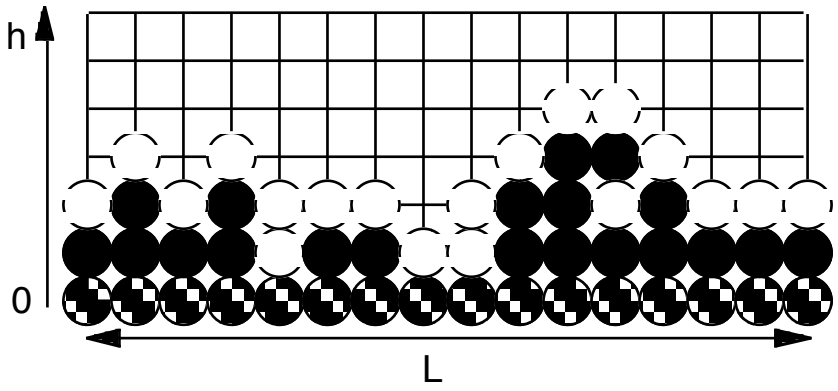

Fig. 4.1.2. Growth of an Eden cluster from a nucleation line (shaded sites).

Because of the global symmetry that is present, we know immediately that, if the surface structure is fractal, it has every chance of being a self-affine fractal, since the direction of growth, h, plays a very different role to the other directions (x, y, etc.), parallel to the line or surface of nucleation. The mean

height of the cluster, $\langle h \rangle$, is simply the mean of the lengths h_i of the n_s points on its surface:

$$\boxed{\langle h \rangle = \frac{1}{n_s} \sum_i h_i} \quad . \tag{4.1-1}$$

We could equally well take the mean height as $\bar{h} = N/L$, where N is the number of particles in the cluster, because, owing to the dense nature of the cluster, $\langle h \rangle$ and $\bar{h}$ very quickly converge to one another as $N \to \infty$.

Note that if the nucleation sites are excluded, N coincides with the time n (remember we assumed a constant rate of sticking here), and consequently both $\langle h \rangle$ and $\bar{h}$ vary linearly with time *for large enough values of N*.

Another important quantity (related to the extent of the surface's roughness) is the mean thickness of the surface defined by the variance of the height

$$\boxed{\sigma^2 = \frac{1}{n_s} \sum_i (h_i - \langle h \rangle)^2} \quad . \tag{4.1-2}$$

4.1.1 Growth of the Eden cluster: scaling laws

When growth takes place from an initially flat surface, two types of behavior may be observed according to whether the mean height is greater or smaller than a critical height, $\langle h \rangle_c$, which depends on the width of the sample, L. The initially flat surface of the cluster becomes increasingly rough (σ increases with time, i.e., with $\langle h \rangle$). This continues until fluctuations in the value of h become sufficiently large in relation to the sample width, L, at which point these fluctuations group around a value dependent on L. An interesting aspect of these growth models is that they possess scaling laws, a property which we have found repeatedly in fractals, Brownian motion, fronts, etc.

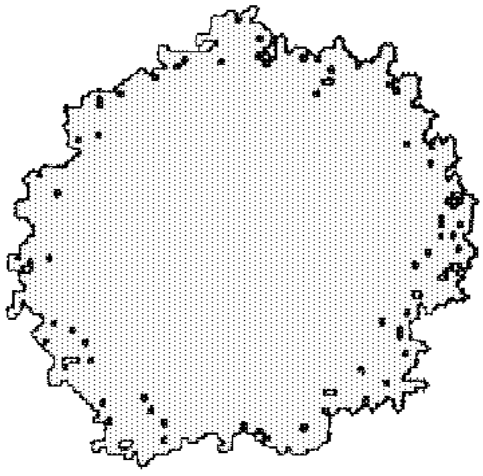

Fig. 4.1.3. Eden cluster composed of 1500 occupied sites generated from a seed (H.J. Herrmann, 1986).

Thus, the crossover point between régimes depends on L via a power law:

$$\langle h\rangle_c \propto L^z . \tag{4.1-3}$$

Which of the two regimes occurs depends on whether $\langle h\rangle$ is smaller or larger than $\langle h\rangle_c$:

$$\sigma(L,\langle h\rangle) \propto \langle h\rangle^\beta \text{ when } \langle h\rangle << L^z, \tag{4.1-4a}$$

$$\sigma(L,\langle h\rangle) \propto L^\alpha \text{ when } \langle h\rangle >> L^z. \tag{4.1-4b}$$

Here, $\langle h\rangle_c$ plays the role of a characteristic length for the system, hence we should expect there to be scaling laws involving the ratio $\langle h\rangle/\langle h\rangle_c$. Numerical calculations confirm that for large enough values of h and L (presence of scaling law behavior), σ takes the general form

$$\boxed{\sigma(L,\langle h\rangle) \approx L^\alpha \; f\left(\frac{\langle h\rangle}{L^z}\right)} \; ; \tag{4.1-5}$$

the function f being such that

$f(x) \propto x^\beta$ as $x\to 0$, where $\beta=\alpha/z$ [to satisfy Eq. (4.1-4a)]
and $f(x)\to$ const. as $x\to\infty$ [to satisfy Eq. (4.1-4b)].

Note that we could equally well express the evolution of the thickness, σ, in terms of a scaling law involving time: the system is flat at $t = 0$ ($\langle h\rangle = 0$), and since $\langle h\rangle$ is proportional to t,

$$\boxed{\sigma(L,t) \approx L^\alpha \; f\left(\frac{t}{\tau}\right)} \, , \tag{4.1-6}$$

where $\tau \propto L^z$ is the characteristic time for a transitory régime to change to a stationary régime. These power laws and this scaling law, which not only involve the geometry of the system but also time, are called *dynamical scaling laws*.

Numerical results show that in dimension d = 2,

$$\begin{aligned} \alpha &\cong 0.5, \\ \beta &\cong 0.33, \\ \text{and hence } z &\cong 1.5. \end{aligned} \tag{4.1-7}$$

Similar numerical calculations in $d > 2$ are difficult. This is due to the fact that the surface thickness, σ, is composed of two terms, one of these σ_{sc} (scaling) follows the scaling law above, the other σ_i is an quantity intrinsic to the model and is independent of L: $\sigma^2 = \sigma_{sc}^2 + \sigma_i^2$. This intrinsic contribution arises from the fact that new growth sites have the same chance of being occupied as the older ones; when $d > 2$ this prevents the values of the exponents α and β being found with any great accuracy. This effect may partially be eliminated by employing a *noise reduction* method. A counter set to zero is placed at each new growth site. Each time a site is chosen, its counter is

incremented by one unit. When the counter reaches a predetermined value m, the site finally becomes occupied,[1] thus ensuring that the oldest growth sites have the highest probability of becoming occupied first. This reduces the intrinsic fluctuations, σ_i, without changing the exponents α and β (which are related to σ_{sc}) (see Fig. 4.1.4).

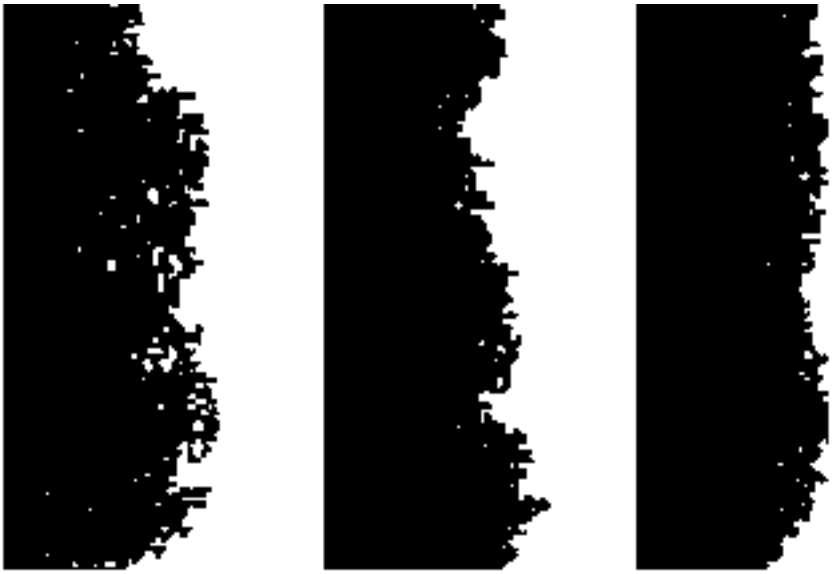

Fig. 4.1.4. Eden surfaces generated using three different values of the noise reduction parameter: from left to right, m=1, m=2, m= 4. This parameter corresponds to the number of times a site must be chosen for it to become occupied; the larger the value of m is, the more are the local fluctuations reduced (after Kertész and Wolf, 1988).

The results obtained by Wolf and Kertész in 1987 are as follows:

$$\begin{array}{lll} d = 2: & \beta = 0.33 \pm 0.015, & \alpha = 0.51 \pm 0.025, \\ d = 3: & \beta = 0.22 \pm 0.02, & \alpha = 0.33 \pm 0.01, \\ d = 4: & \beta = 0.15 \pm 0.015, & \alpha = 0.24 \pm 0.02. \end{array} \qquad (4.1\text{-}8)$$

These results are in good agreement with the conjecture, which is based on theoretical arguments, that $\alpha + z = \alpha + \alpha/\beta = 2$ (see Sec. 4.3).

We have seen that the body of a cluster produced in this way is *not* fractal. What can be said about the structure of its surface, inasmuch as it is known to exhibit power law behavior?

The self-affine character of the surface of an Eden cluster

At a given moment, the surface of an Eden cluster contains overhangs. That is to say, the height h is not a single-valued function of the abscissa r ($0 \le r \le L$) along the whole of the nucleation line (or of $\vec{r}$ in the case of a

[1] Thus creating new growth sites at which the counter is reset to zero.

nucleation plane). It can, however, be numerically verified that these overhangs play no role in the scaling laws; in other words, the surface defined by the highest occupied sites [of ordinate $h(\vec{r}) = \max(h)$ at a given $\vec{r}$] possesses the same characteristics as the whole surface. Therefore, as regards those properties which relate to its large scale geometry, the surface may be represented by a single-valued function $h(\vec{r})$. If the surface is self-affine, we can calculate the auto-correlation function of the heights, as we did in Sec. 2.2.4, Eq. 2.2-8,

$$C(r) = \langle\, [h(\vec{r}_0+\vec{r}) - h(\vec{r}_0)]^2 \,\rangle .$$

Thus, we should expect to find that

$$C(r) \propto r^{2H} , \tag{4.1-9}$$

where H is the Hurst exponent of the self-affine structure. Moreover, comparison with the previous results requires that $H = \alpha$. The thickness is found by calculating

$$\sigma^2 = \langle\, [\, h(\vec{r}_0) - \langle h(\vec{r}_0)\rangle\,]^2 \,\rangle = \langle\, [\, h(\vec{r}_0)]^2 \,\rangle - \langle h(\vec{r}_0)\rangle^2 ,$$

and so, when the heights are uncorrelated, C(r) becomes

$$C(r) = \langle\, [h(\vec{r}_0 + \vec{r}\,) - h(\vec{r}_0)]^2 \,\rangle = 2\left(\langle\, [\, h(\vec{r}_0)]^2 \,\rangle - \langle h(\vec{r}_0)\rangle^2\right) = 2\sigma^2 .$$

There is no correlation when r is sufficiently large (i.e., larger than a distance corresponding to the correlation parallel to the nucleation plane), which is the case when r = L. Hence (and this result has been well confirmed numerically),

$$C(L) = 2\,\sigma^2 \propto L^{2\alpha} \quad \text{et} \quad H = \alpha. \tag{4.1-10}$$

So, the surface of an Eden cluster is a self-affine structure, its local fractal dimension is given (cf. Sec. 2.2.4) by $D = d - \alpha$.

The Eden model is the simplest growth model. Several attempts to find an analytic solution have been made. Edwards and Wilkinson (1982) constructed a model which, by including nonlinear terms to take account of the irreversible nature of growth, achieved reasonably good values for the exponents, namely $\alpha = 1/2$ and $z = 3/2$. Subsequently, this equation was refined by Kardar, Parisi, and Zhang (1986); we shall return to this analytic approach when we come to look at deposition models in Sec. 4.3.

Certain features of the Eden model clearly demonstrate the difference that exists between an irreversible kinetic process and a critical phenomenon. For example, the lattice configuration may affect the structure: in a square lattice the cluster issuing from a nucleation site progressively acquires a diamond shape (however, this requires a large amount of computing time and more than 10^9 particles).

4.1.2 The Williams and Bjerknes model (1972)

This generalizes the Eden model by allowing a growth site neighboring a malignant cell to be contaminated with probability α and this malignant cell to become healthy with probability β.

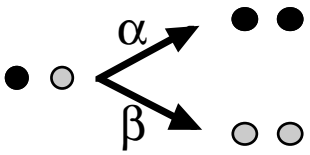

The important parameter here is the ratio $\kappa=\alpha/\beta$.

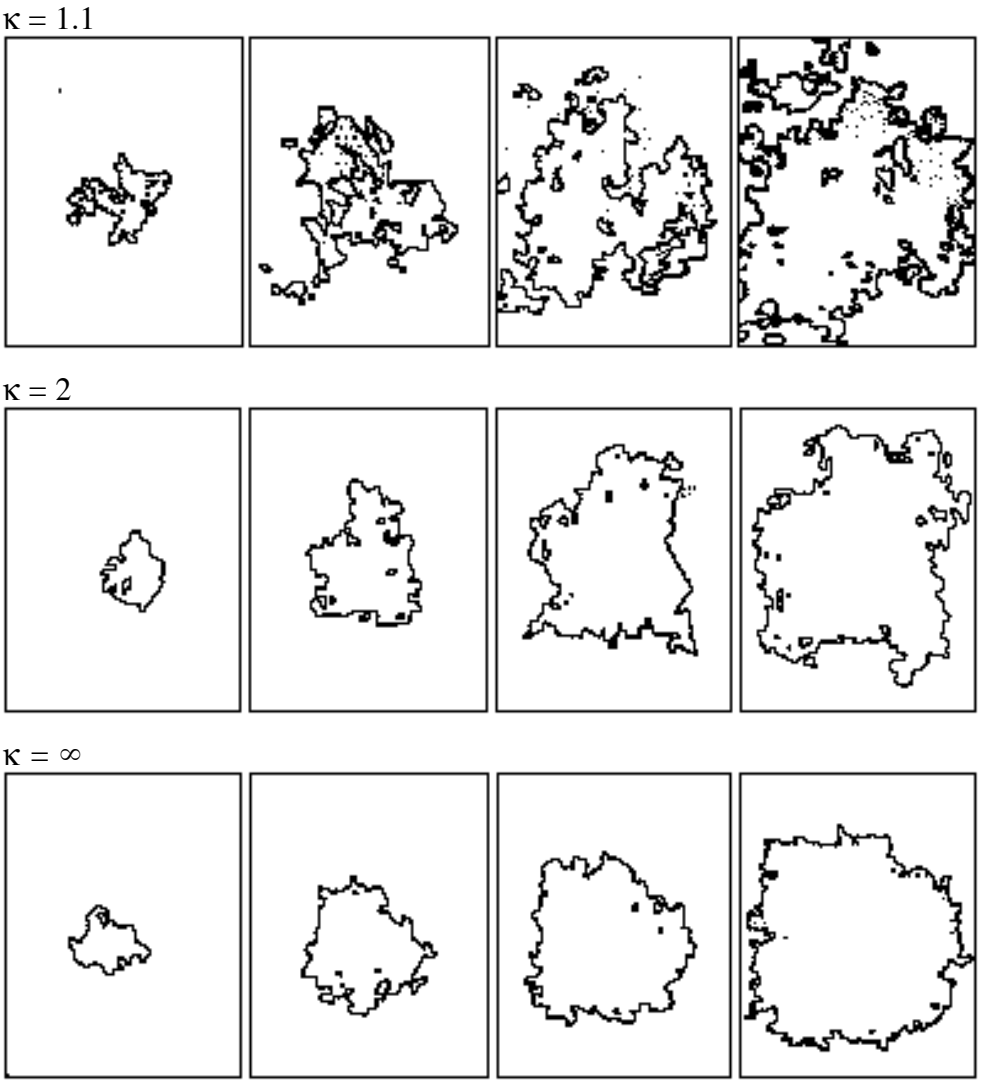

Fig. 4.1.5. Clusters obtained from the Williams and Bjerknes model for three values of the ratio α/β. The value $\kappa=\infty$ corresponds to the Eden model. (Williams and Bjerknes, 1972).

If $\kappa > 1$, the contagion spreads. As with the Eden model, we find clusters of dimension d and self-affine surfaces (Fig. 4.1.5). There are very good reasons

to think that this model belongs to the same universality class as the Eden model, and that, up to a scaling change (depending on κ), their clusters are similar.

4.1.3 Growth of percolation clusters

The Eden model may also be modified in the following way: a growth site G may be contaminated by a sick neighboring cell (occupied site of the cluster), but then only a proportion p of these sites G develop the illness and go on to contaminate their other neighbors, while the remaining $(1-p)$ become immunized and are no longer growth sites (Fig. 4.1.6). The case $p=1$ corresponds to the Eden model.

This model is of great interest, because it is a growth model which generates percolation clusters. It is comparable to the invasion percolation model described in Sec. 3.2.3, but which could just as well have been included in this chapter. The two models are, in fact, different since, in invasion percolation, growth is never blocked and the proportion p of invaded sites progressively increases from zero until it approaches the value p_c; the invaded region thus becomes the incipient percolation cluster.

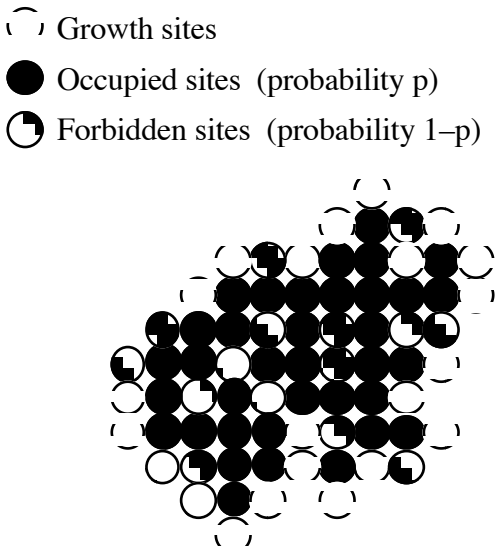

Fig. 4.1.6. Percolation cluster growing from a seed (heavily shaded); the cluster sites are shown in black, the forbidden (immunized) sites are shaded.

In the growth model examined here:

If $p < p_c$, the cluster develops until, at a certain moment, it reaches a finite size for which there are no more growth sites available (the perimeter being composed of immunized sites).

If $p > p_c$, an infinite cluster develops: the "contagion" has then spread a great distance.

When the growth stops, the cluster obtained is *identical* to a percolation cluster. However, *while the growth is in progress*, this is not at all the case: the cluster has the same fractal dimension as a percolation cluster, but globally it is less anisotropic, and its perimeter (growth sites) bears no relation to that of a percolation cluster.

4.2 The Witten and Sander model

4.2.1 Description of the DLA model

The Witten and Sander, or diffusion-limited aggregation (DLA), model is without doubt the most important particle–cluster aggregation model. It was proposed in 1981 by Witten and Sander and has since been the starting point for a great number of studies. The initial motivation was to explain the experiments of Forrest and Witten on the aggregation of smoke particles, but, as it turned out, the model applies much better to a different class of phenomena, as we shall see later. The model works as follows:

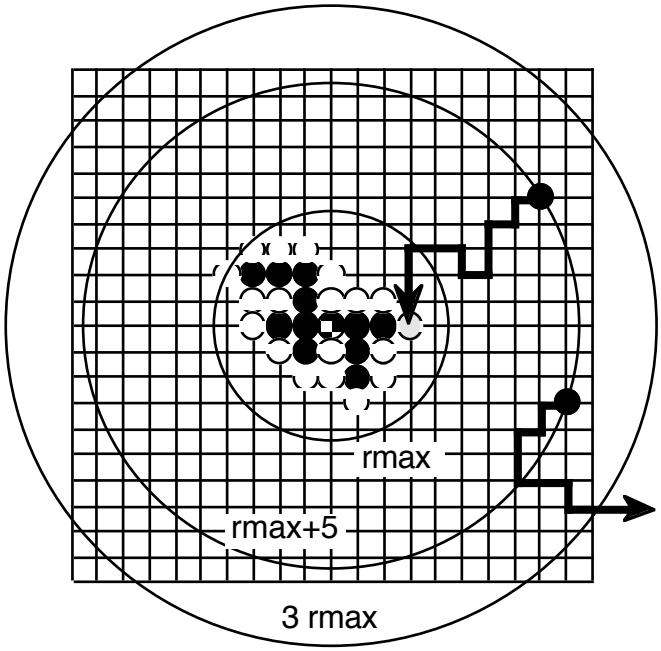

Fig. 4.2.1. Diagram of the DLA model on a square lattice. Growth takes place from a seed (hatched). The cluster sites are shown in black, the growth sites in white. The figure shows the trajectories of two particles, one of which drifts too far from the cluster and is lost.

Particle *n* diffuses through a lattice from a point of which, situated in an arbitrary direction far away from the developing cluster, it originates. When the particle arrives in contact with the cluster, it sticks *permanently*. Then particle *n+1* arrives, and so on. *In practice*, the numerical simulation is carried out following the scheme shown in Fig. 4.2.1: to prevent the computation time from being prohibitively long, the *n*th particle is positioned at random at a distance of the order of $r_{max} + 5$ from the cluster, where r_{max} is the distance of the furthest point from the initial germ. This has no effect on the future evolution of the system as the particle's *first encounter* with a circle not intersecting the cluster is equally likely to occur at any of its points. In addition, certain particles may wander too far from the cluster (and in $d \geq 3$ do so irreversibly). It may be assumed, but this is of course only an approximation, that the role of the departure point has sufficiently diminished at $r = 3\ r_{max}$, and that it would waste too much computation time waiting for it to return towards the cluster (in three dimensions there is even a nonzero probability that we would wait forever!). When this happens we start again with a new particle. A random walk over the lattice simulates Brownian diffusion. Aggregates may also be constructed without the use of a lattice. Fig. 4.2.2 displays an aggregate from the Witten and Sander model (here of 50,000 particles) generated off-lattice.

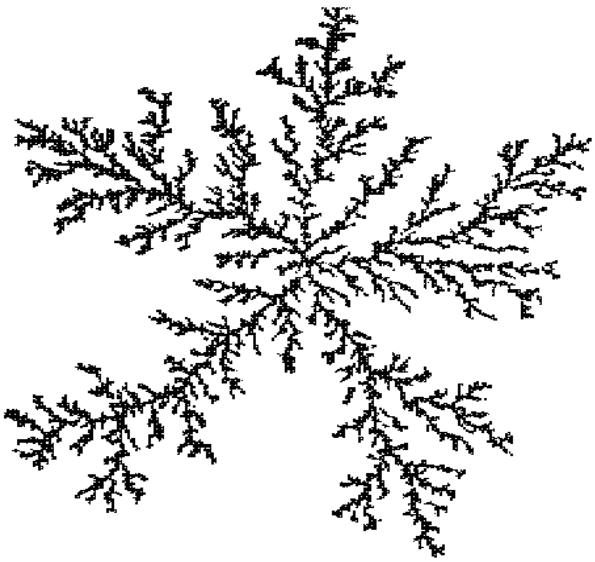

Fig. 4.2.2. Example of an off-lattice DLA cluster [2] composed of 50,000 particles. The fractal dimension is found to be close to 1.71 (Feder, Fractals, 1988).

[2] In off-lattice diffusion, each particle moves with equal probability to any point one particle diameter away. When it touches a cluster particle during this motion, it sticks to the cluster.

In principle, the fractal dimension does not depend on the lattice but only on the Euclidean dimension d. By contrast, as with the Eden model, the global shape of the cluster is sensitive to the lattice: with a square lattice, the cluster takes on a shape with four petals, as is more clearly demonstrated when noise reduction is used (see, e.g., Meakin and Tolman in Pietronero, 1989). Whereas the fractal dimension is close to D = 1.715 in the off-lattice model, it appears to be close to 1.5 for a square lattice, which, as we might expect, introduces two exponents (longitudinal and transversal), as did the Eden model.

Table V below gives the values of the fractal dimension D, for $1 < d \leq 6$. No exact analytic expression for D(d) is known. Mean field arguments produce a good approximation to the fractal dimension

$$D(d) = (d^2 + 1)/(d + 1).$$

Table V: Numerically obtained fractal dimensions of the DLA cluster in various spatial dimensions (Meakin,1983)

d	2	3	4	5	6
D	1.71	2.53	3.31	4.20	5.3
$(d^2+1)/(d+1)$	1.67	2.50	3.40	4.33	5.29

4.2.2 Extensions of the Witten–Sander model

Two types of extension are of physical interest. The first consists in allowing a probability of sticking other than 1. When the diffusing particle arrives in the neighborhood of a particle in the aggregate, there is now only a probability $p < 1$ of sticking taking place. The sticking, however, remains irreversible (when the particle crosses the sticking barrier it is trapped permanently). This model simulates a diffusion-reaction process.

In this model a *crossover* occurs. After a long time has elapsed and the cluster is reasonably large, the fractal dimension is independent of p and identical to that of the Witten and Sander aggregate just studied above. In contrast, at the start of the aggregation process, the cluster appears more compact. In particular as $p \to 0$, it takes on the appearance of an Eden model aggregate. It is easy to see the reason for this: as $p \to 0$ the particle visits a large number of sites neighboring the aggregate before it finally sticks. So, the probability of sticking to each of them is practically the same, and this approximately defines an Eden model. For any given value of p, after N of the sites neighboring the cluster have been visited, the probability of an (N + 1)th site being visited is no greater than $(1 - p)^N$. When the cluster has grown large, the sites with a non-negligible chance of being visited are limited to a small neighborhood of the point of first contact and we find ourselves in a scenario similar to the Witten and Sander model.

Another interesting extension consists in modifying the mean free path of the diffusing particle. In the Witten–Sander model, the mean free path is the distance between sites. In many aggregation processes (especially in gaseous phases), this mean free path, Λ, need not be negligible, and here again there is a crossover. If we suppose Λ to be infinitely large, then the regime is *ballistic*, the particles randomly describing directed straight lines in space. (This model was introduced by Vold in 1963.) Recent numerical calculations have given values for the fractal dimension of 1.93 and 1.95, and it is almost certain that in two dimensions the true value is 2. Similarly in three dimensions a value of 2.8 is found, but the true value is most probably 3: *the aggregates formed are compact*. For a finite value of Λ, we find locally compact aggregates up to a range Λ, then beyond this we pass to a Witten–Sander type structure. The purely ballistic case where the particles arrive from a single direction is a model for deposition; it generates rough, self-affine surfaces (see Sec. 4.3).

Many physical systems involving aggregation (which were mentioned above in the section on aggregation in a field) can be modeled by the DLA model. This is due to the fact that, roughly speaking, all of these systems turn out to be solutions to Laplace's equation.

Consider a particle diffusing in the DLA model before it sticks to the cluster. The probability, P, of finding the particle at position r is found by solving a diffusion equation:

$$\frac{\partial P(\vec{r}, t)}{\partial t} = \mathcal{D}\, \Delta P(\vec{r}, t)\ , \tag{4.2-1a}$$

where $\mathcal{D}$ is the diffusion coefficient. The boundary conditions are as follows:

— at a large enough distance (r_{ext}) from the cluster the particle has a uniform probability:

$$P\ (\vec{r}_{\,ext}, t) = P_0\ ; \tag{4.2-1b}$$

— when the particle reaches the cluster it is adsorbed, and the probability of it penetrating inside the cluster is zero:

$$P\ (\vec{r} \in \text{cluster}, t) \equiv 0. \tag{4.2-1c}$$

If we take sufficiently long intervals of time to allow each particle to reach the cluster, then the aggregation process is approximately in a steady state, since the addition of a small number of particles to the cluster does not appreciably alter its structure. Therefore, to find the probability of a diffusing particle being at a given point, we have to solve (steady state)

$$\Delta P(\vec{r}, t) = 0\ , \tag{4.2-2}$$

with the boundary conditions above [Eqs. (4.2-1b) and (4.2-1c)].

If the more practical model shown in Fig. 4.2.1 is employed, the problem is more subtle, since, as the particles are eliminated at $3r_{max}$, the probability there is nil as it is in the cluster. If we use a uniform distribution of starting sites at $r_{max} + 5$ to

calculate the probability distribution (which satisfies $\Delta P = 0$), we find that it reaches a maximum at an intermediary distance and that its equipotentials (P = constant) are still practically circular far from the cluster. By contrast, the starting sites at $r_{max} + 5$ are too close to the cluster to be equipotential. But viewed from a neighborhood of the cluster it appears as though the particles have originated from a uniform circular source situated far away.

The particle current is given by the gradient field, grad $P(\vec{r})$. As this gradient field is related to the local curvature of the surfaces of equal probability (equipotentials), the tips grow more rapidly than the fjords. We shall see that these remarks also apply to the examples in Sec. 3.4.5. First of all, it is important to stress here the role played by random fluctuations. Let us suppose that we solve Eqs. (4.2-1) by allowing the initially linear cluster to grow at a rate proportional to grad $P(\vec{r})$. The surface of the aggregate will then remain flat, but this situation is metastable and the least curvature will immediately develop a tip. Random fluctuations in the process of particles sticking one at a time to the cluster (DLA), or in the distribution of pore diameters or in the local probabilities of dielectric breakdown, thus play a crucial role in the growth of ramified fractal structures, by continually destabilizing the process and preventing it from being regular.

In this regard, it is instructive to see how the different wavelengths at the start of the process develop when the linear approximation is still valid. If we start with a structure with a small surface oscillation of wavelength λ, it will develop fairly quickly. In general there is a critical wavelength λ_c, such that for $\lambda > \lambda_c$ the wave front is unstable, while for smaller wavelengths it is damped. For instance, in the case of injection (viscous fingering), $\lambda_c \approx \sqrt{C_a}$ [Eq. 3.2-5], the fastest developing wave front having wavelength $\lambda_m = \sqrt{3}\,\lambda_c$.

Electrolytic deposition

Here, the circular anode is set at a potential V_0, the cathode (germ) being set at zero potential. Ions diffuse in the presence of an electric field which is stronger the nearer they approach a deposition point, where they will be reduced. Growth is thus more rapid in the vicinity of tips (Fig. 3.4.10). We can see immediately that when the conditions are such that the current is too weak for nonlinear or dynamic effects to occur, that is, when the ion concentration is low enough, electrolytic deposition is very similar to a DLA situation, provided that the sticking is immediate. However, this type of growth is still only very incompletely understood due to some complicated problems of electrochemistry. Moreover, the carrier fluid is not immobile but animated in the neighborhood of the points of hydrodynamical motion, and governed by a Navier–Stokes equation (see, e.g., Fleury et al., 1991).

Dielectric breakdown

Dielectric breakdown (Fig. 3.4.11) also belongs to the DLA family. To see this, we must look more closely at the growth model of this breakdown. Locally there is a discharge between neighboring molecules, which may be thought of as a cluster of low resistance bonds that close at each discharge (a plasma of ionized molecules is formed). Once a discharge has occurred between two molecules, the conductivity takes a higher value. New ruptures create links to the periphery. In an insulator, the Laplace equation is always satisfied, and the probability of discharge is proportional to the gradient at the discharge surface (as with DLA), or, more generally, to a *power of the gradient* there (DLA variant: Niemeyer, Pietronero, and Wiesmann model discussed below).

Injection into a porous medium

Here a fluid of low viscosity (i.e., with a large capillary number C_a, see Sec. 3.2.3) is injected into a porous medium. In experiments where a fluid is forced into another more viscous fluid, the *potential* represents the pressure, and the *field* represents the velocity field. For an incompressible fluid satisfying Darcy's law, the current, $\vec{v}$ (flux per unit normal surface area, see Sec. 3.2.1), is proportional to the pressure gradient, P,

$$\vec{v} = -\alpha \ \overrightarrow{\text{grad}}\, P. \qquad (4.2\text{-}3)$$

The conservation constraint div $\vec{v} = 0$ leads again to $\Delta P = 0$. The boundary conditions at the interface are only consistent with the DLA model when the viscosity of the injected fluid is negligible compared to that of the displaced fluid. In the experiment shown in Fig. 3.4.12, Daccord and his colleagues measured the dimension to be $D = 1.7 \pm 0.05$.

Laplacian fractals

The term "Laplacian fractals" (Lyklema, Evertsz, and Pietronero, 1986) is used to describe fractals that have been obtained from diffusion-limited aggregation processes, that is, those which model critical kinetic phenomena governed by the Laplace equation. The components are, as we have just seen, the Laplace equation together with a law indicating how the kinetics are related to this equation (Fick equation) and a random component. The Fick equation determines the probability current, while the random element (here the individual random motion of a particle) allows the fractal cluster to grow by constantly changing (at each sticking) the boundary conditions, in a process which is in fact very far from equilibrium. If we attentuate this random element by allowing a large number of particles to diffuse simultaneously, the Laplace equation will be satisfied but no fractal structure will be generated (more precisely, its development will be slowed down considerably, as when m is chosen very large in the noise reduction of Sec. 4.1.1). The kinetics of the diffusing particle's random walk may be subjected to a particular constraint to help better model a physical process, for example dielectric breakdown.

Niemeyer et al. (1984) have studied the growth of Laplacian fractal structures for which the probability of growth satisfies the equation

$$P(i \to j) = \frac{|V(i) - V(j)|^{\eta}}{\sum_{i,j} |V(i) - V(j)|^{\eta}} \quad , \tag{4.2-4}$$

i being a cluster site at potential V(i) = 0, j a growth site, and P(i $\to$j) the probability (normalized to one) of occupying site j starting from site i.

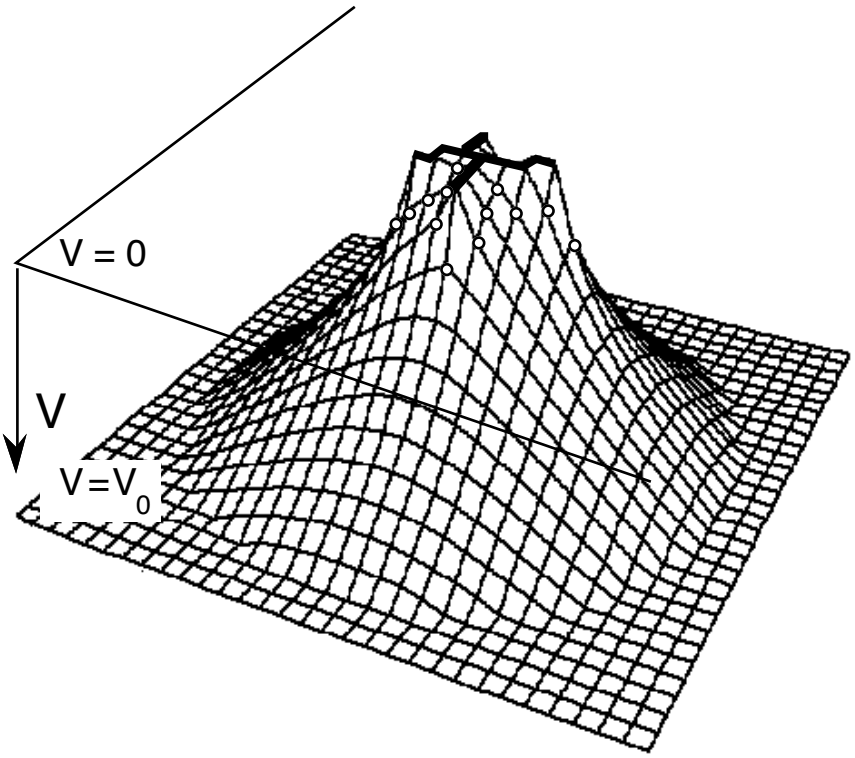

Fig. 4.2.3. Diagram representing the potential between a circular electrode at potential V_0 , ($V_0 > 0$), and an aggregate or an earthing point at potential $V = 0$ (indicated by a thick black line). Equivalently, this potential V represents the probability density P of a particle, originating at the boundary, being found at a given point. The probability current is given by Fick's law $\vec{J} = -\mathcal{D}\ \overrightarrow{grad}\, P$. The points adjacent to the cluster (white circles) are the growth sites. The probability of their being occupied is greater, the smaller is their ordinate (larger gradient), which is precisely the case for the tips of the cluster. In the case of electrical discharge, Niemeyer et al. have proposed that the probability of discharge between neighboring molecules is proportional to a power η of the electric field, that is, $\vec{J} = -\mathcal{D}\ (\overrightarrow{grad}\, V\ )^{\eta}$

The V(j)'s are calculated by solving the Laplace equation each time a new particle is added. The potential profile is shown in Fig. 4.2.3. The tips are in a

stronger field and grow more quickly. For $\eta = 1$, we get a DLA cluster, although the microscopic process is different. Finally, for $\eta = 0$ we get an Eden cluster (equal probability for each growth site).

All these fractal structures are *self-affine*.[3] This is easier to see if the growth takes place from a line or a plane, as in Fig. 3.4.13 (see also Evertsz, 1990).

4.2.3 Harmonic measure and multifractality

During the growth of a DLA cluster, as we have already noticed, the growth sites are not occupied with the same probability. Growth sites situated on the tips of cluster branches have a higher than average weighting, while there are sites, situated at the ends of fjords formed by the branches, whose probability of being occupied is practically nil (Fig. 4.2.4). It is important to characterize this probability distribution, as it is directly involved in the growth of the cluster. Such a characterization does exist and uses multifractility.

In the case at hand, we give the following sketch of this multifractal approach. Suppose that we wish to investigate the charge distribution on a charged conductor of any shape placed in a vacuum. To do this we would have to solve the Laplace equation with boundary conditions $V = V_0$ at infinity and $V = 0$ on the conductor. For a surface element dS of charge dq, the surface charge density is $\sigma = dq/dS$, and the electric field, E_n, normal to the surface in the immediate neighborhood of the conductor is given by

$$E_n = \sigma/\varepsilon_0 \ . \tag{4.2-5}$$

The potential V_0 is also related to the charge distribution:

$$V_0 = \frac{1}{4\pi\varepsilon_0} \int \frac{dq}{r} \ . \tag{4.2-6}$$

The charge distribution on the surface of the conductor is called the *harmonic measure* (this name comes from the fact that Laplace's equation is satisfied by harmonic functions).

Thus, the problem of cluster growth is related to the notion of harmonic measure. For example, in the electrostatic problem associated with the DLA model, or with Laplacian growth, we have just seen that the probability $G(\vec{r})$ of a growth site being occupied, as a function of $\vec{r}$, is given by a power law in the electric field E_n and so also of σ ($\eta = 1$ for DLA):

$$G(\vec{r}\,) = \frac{E_n(\vec{r}\,)^{\eta}}{\int_S d\vec{r}\, E_n(\vec{r}\,)^{\eta}} \ . \tag{4.2-7}$$

[3] In the case of DLA, however, each branch appears to be self-similar.

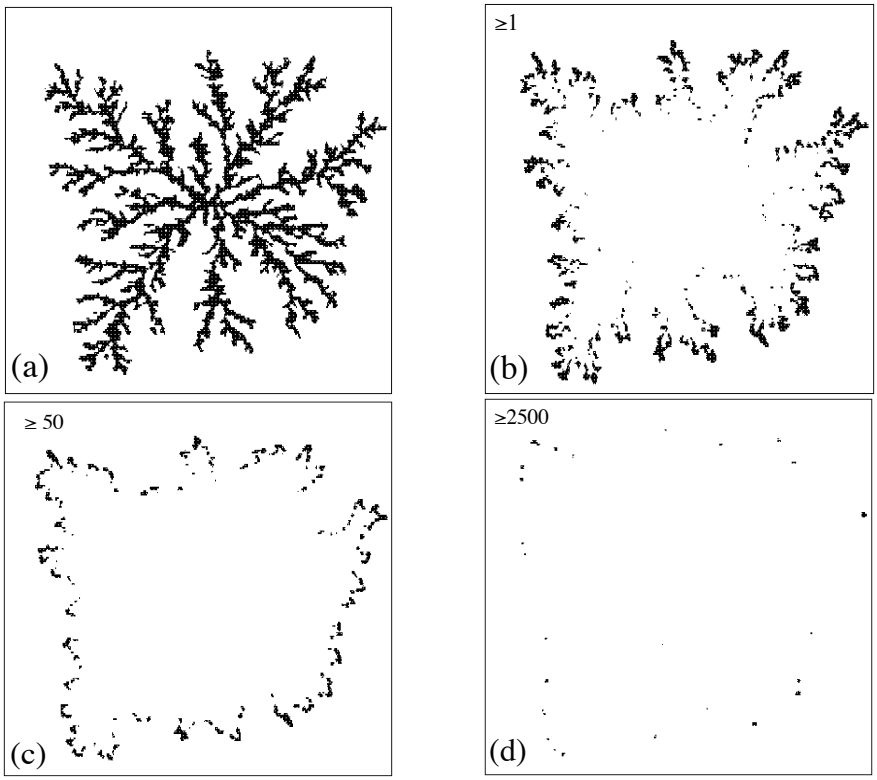

Fig. 4.2.4. Having constructed an off-lattice DLA cluster of 50,000 particles (a), we would like to know the probability distribution for the sticking of the 50,001th. To do this, a large number (10^6) of random walks are simulated and the number of times that the 50,001th diffusing particle comes into contact with each of the cluster particlest is determined. Figures (b), (c), and (d) show the particles which have been touched more than once, more than 50 times, and more than 2,500 times respectively (Meakin et al., 1986).

Unfortunately, it has not yet been possible to study the multifractal structure that corresponds to the harmonic measure for a DLA cluster analytically. If a is the size of a particle cluster, then (see Sec. 1.6, especially Sec. 1.6.4)

$$M_q(\varepsilon = \frac{b}{L}) \equiv \int_S d\vec{r}\ G\left(\frac{b}{L}, \vec{r}\right)^q = b^{1-q}\ \left(\frac{b}{L}\right)^{-\tau(q)}, \qquad (4.2\text{-}8)$$

where $b = \varepsilon L$ ($\varepsilon << 1$) is the size of the boxes centered at the different points $\vec{r}$, and $G(\varepsilon,\vec{r})$ is the cumulative probability (i.e., the measure inside a box). We can also fix b and vary the cluster size L to study the effect of increasing this size.

Knowing $\tau(q)$, the function $f(\alpha)$, which characterizes the multifractal structure, may then be found. This function achieves a maximum D_0 which is the dimension of the support of the measure, that is, the dimension of the DLA cluster itself: $D_0 \cong 1.71$. In their numerical calculations, Hayakawa et al. (1987) found $D_0 \cong 1.64$ and $D_1 \cong 1.04$.

In two dimensions, a theorem of Makarov (1985) and Jones and Wolff (1988) states that the information dimension of the harmonic measure is exactly equal to one. This means that the fractal dimension of the support containing the majority of the charge is $D_1 = 1$, whatever the shape of the conductor (which is in good agreement with above). It has also been conjectured that in three dimensions the information dimension is equal to 2.5.

4.3 Modeling rough surfaces

We have already spoken implicitly (Sec. 3.4.1) about two growth models for rough surfaces: the Eden model (explained in Sec. 4.1) and ballistic aggregation. Of course, not all rough surfaces can be described by these two models alone; examples of those than cannot include surfaces generated by fractures, mentioned in Sec. 2.2.9.

4.3.1 Self-affine description of rough surfaces

The term "rough surface" defines an irregular surface in which there are no overhangs, or rather, in which *such overhangs do not dominate the scaling properties*. When these conditions are obtained, a rough surface may be correctly described by a function $h(\vec{r})$ which specifies the height[4] of the surface at position $\vec{r}(x,y)$ on an appropriate reference plane (in $d = 3$). For a mountain relief, the reference plane is mean sea level, and $h(\vec{r})$ is the altitude at the location $\vec{r}$ (defined by its latitude and longitude). For a great many rough surfaces occurring in nature, this function $h(\vec{r})$ is characteristic of a *self-affine fractal structure*. The growth of such a structure may thus be characterized by means of the parameters $\langle h \rangle$ and σ defined in the Eden model.

4.3.2 Deposition models

Deposition processes (from a vapor, by sedimentation, etc.) represent typical cases of the growth of rough surfaces. Clusters produced by deposition are dense, only their surfaces have an irregular structure. Various models have been studied in the last few years (a recent review can be found in Family, 1990, which we follow here). Here, we shall describe only three models: *random deposition*, *random deposition with diffusion*, and *ballistic deposition*.

Random deposition is the most elementary of these models. Here the particles fall vertically at random onto a horizontal substrate and pile up along

[4] If there are overhangs in the surface, we take $h(\vec{r}) = \max(h)$ at position $\vec{r}$.

each vertical line (Fig. 4.3.1). The heights $h(\vec{r})$ are thus uncorrelated and follow a Poisson distribution, so that whatever the value of d,

$$\begin{aligned} &\langle h\rangle \propto t \\ \text{and} \qquad &\sigma \propto t^{1/2} \ . \end{aligned} \tag{4.3-1}$$

The process does not depend on the sample size L.

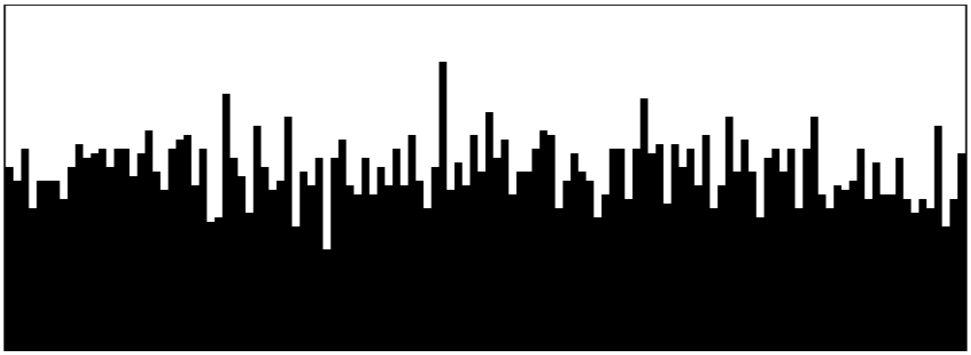

Fig. 4.3.1. Random deposition onto a one-dimensional substrate (d = 2) (Family, 1990).

Random deposition with surface diffusion is identical to the previous model except that instead of sticking immediately to the cluster, the particles "diffuse" before stabilizing at a more stable site situated within a given radius (the particles roll down into the holes) (Fig. 4.3.2). In this model restructurization is dominant; the rough surface generated now depends on the sample size. It behaves much like an Eden model, but belongs to a different universality class (i.e., its exponents have different values). In particular, the surface fluctuations obey a scaling law of the form

$$\boxed{\sigma(L,\langle h\rangle) \approx L^{\alpha}\ f\left(\langle h\rangle / L^{z}\right)} \ , \tag{4.3-2}$$

where, as with the Eden model, the function f is such that

$$\begin{aligned} &f(x) \to \text{const.} \quad \text{as } x \to \infty \\ \text{and} \qquad &f(x) \propto x^{\beta} \quad \text{as } x \to 0, \ \text{where } \beta = \alpha/z. \end{aligned} \tag{4.3-3a}$$

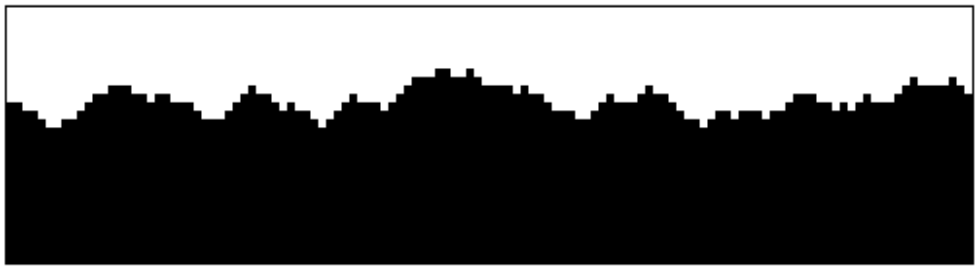

Fig. 4.3.2. Random deposition with diffusion (d = 2) (Family, 1990).

By adopting an analytic approach that uses Langevin's equation (Sec. 4.3.3), Edwards and Wilkinson (1982) have proposed the following relations:

$$\alpha = (3 - d)/2, \quad \beta = (3 - d)/4, \quad \text{and} \quad z = 2. \tag{4.3-3b}$$

The fractal dimension of this self-affine surface (with Hurst exponent $H \equiv \alpha$) is thus

$$D = d - \alpha = 3(d - 1)/2. \tag{4.3-3c}$$

Ballistic deposition: we have already spoken earlier about ballistic aggregation (Sec. 4.2.2). In this model introduced by Vold (1959), the direction in which the particles fall is normal to the substrate, and when they enter into contact with one of the cluster particles they stick there permanently (Fig. 4.3.3). Again the general behavior is very similar to that of the Eden model. Numerical studies lead to the following predictions concerning the scaling laws of the surface:

$$\sigma \propto t^{\beta}, \quad \text{where } \beta \cong 1/3 \text{ in } d = 2. \tag{4.3-4a}$$

Finite size effects also occur,

$$\sigma \propto L^{\alpha}, \quad \text{where } \alpha \cong 1/2 \text{ in } d = 2. \tag{4.3-4b}$$

Fig. 4.3.3. Ballistic deposition along a direction normal to the substrate (Family, 1990).

There is no experimental reason for ballistic deposition to take place perpendicular to the substrate, and ballistic models involving an oblique incidence have been investigated. This leads to columnar structures similar to those observed experimentally. In this case, the exponents α and β vary continuously with the angle of incidence.

4.3.3 Analytic approach to the growth of rough surface

In 1986, Kardar, Parisi, and Zhang proposed an equation governing the variation in height $h(\vec{r},t)$ during the growth of a rough surface. This equation

generalizes the approach developed by Edwards and Wilkinson in their study of random deposition with diffusion. It is a nonlinear Langevin equation,

$$\partial\tilde{h}(\vec{r},t)/\partial t = \gamma\Delta\,\tilde{h}(\vec{r},t) + \lambda\left(\overrightarrow{\text{grad}}\,\tilde{h}(\vec{r},t)\right)^2 + \eta(\vec{r},t) \quad \text{with} \quad \tilde{h} = h - \langle h\rangle \,. \tag{4.3-4}$$

It contains a relaxation term whose coefficient is associated with the surface tension (as does Laplace's equation for an elastic membrane), a nonlinear term corresponding to the lateral growth with coefficient λ (see Vicsek, 1989, p. 200 for further details) and a noise term, η, which allows the introduction of some randomness. In the models that we have just studied this noise is a white Gaussian noise satisfying

$$\langle \eta(\vec{r},t)\,\eta(\vec{r}\,',t')\rangle = 2C\,\delta(\vec{r}-\vec{r}\,')\,\delta(t-t') \,. \tag{4.3-5}$$

The case when $\gamma = \lambda = 0$ corresponds to random deposition with $\beta = 1/2$; if $\gamma \neq 0$, $\lambda = 0$, then we have deposition with restructurization, $\alpha = (3-d)/2$, $\beta = (3-d)/4$, and $z = 2$; finally, in the general case (ballistic deposition and the Eden model), we find for $d = 2$ that $\alpha = 1/2$, $\beta = 1/3$, and $z = 3/2$, which agrees with the numerical results obtained in $d = 2$. The situation remains unclear[5] in $d > 2$.

Let us end this section by adding that the Kardar, Parisi, and Zhang equation is also interesting for the study of other growth models where correlation phenomena intervene (molecular beam epitaxy, for example, can be modeled by random deposition process in which the deposited particles stabilize at sites so as to maximize the number of links, thus introducing a spatial correlation). Recent studies have therefore been led to a modified equation (4.3-4) in which the noise is no longer white but of the form

$$\langle \eta(\vec{r},t)\,\eta(\vec{r}',t')\rangle = 2C\,|\vec{r}-\vec{r}'\,|^{\alpha}\,|t-t'\,|^{\beta} \,. \tag{4.3-6}$$

4.4 Cluster–cluster aggregation

In Sec. 2.7.1 we introduced cluster–cluster processes and gave aerosols and colloids as experimental examples of these processes.

4.4.1 Diffusion-limited cluster–cluster aggregation

In 1983, Meakin and, simultaneously, Kolb, Jullien, and Botet studied the diffusion-limited cluster–cluster aggregation model numerically to characterize the structure of aggregates and the dynamics of their formation. The principle behind the simulation is simple. Initially, a low concentration of particles are randomly distributed over a lattice. The particles diffuse in time by jumping to

---

[5] Kardar et al. have shown, however, that for very large values of λ, it is always the case that
$\alpha + z = 2$.

neighboring sites (double occupation of a site being forbidden) and permanently stick to each other when they touch. The pairs thus formed also randomly diffuse by translation through the inter-site distance, and the clusters stick as soon as they enter into contact with each other. Obviously, there is no reason why clusters of different sizes should have the same diffusion coefficient. For example, we could choose the diffusion coefficient for a cluster of size (mass) s to be

$$\mathcal{D}_s = c\, s^{\gamma} . \tag{4.4-1}$$

Thus, for D-dimensional clusters, taking $\gamma = -1/D$ leads to diffusion coefficients inversely proportional to their hydrodynamic radii (de Gennes, 1979), which for a fractal cluster is of the order of its radius (effective or of gyration).

This aggregation process may be easily generalized to the off-lattice case. As we can see from Table IV in Sec. 3.4.1, the aggregates formed in this way are less dense than those formed by the diffusion-limited particle–cluster process (DLA). This result does not depend on γ so long as $\gamma < 1$ (physically the most common case). When $\gamma >> 1$, this model asymptotically approaches the DLA model, as there are then present only large clusters together with some small clusters that have escaped sticking. Although the large clusters diffuse very quickly here and the small ones remain almost motionless, the relative motion is similar to the DLA case (to convince yourself of this watch the film produced by Kolb, 1986).

The aggregation model can be refined by allowing the clusters to rotate. This does not qualitatively alter the results, or even the internal relaxations of these clusters, but it can lead to a certain restructuring making the clusters denser.

Scaling laws

The size distribution is an important parameter in the description of cluster–cluster aggregation phenomena. It is defined in terms of $n_s(t)$, the mean number of clusters of size s per site at time t. At a given time, the clusters have a mean size $\langle s \rangle(t)$. As with the previous examples involving a scaling régime, we would expect this mean size to obey a power law in time (see for example Vicsek, 1989),

$$\langle s \rangle(t) \propto t^{z} \tag{4.4-2}$$

and there to be be a scaling law of the form

$$n_s(t) \propto s^{-\theta} f(s / t^{z}) . \tag{4.4-3}$$

The exponent θ may be determined by fixing the mean concentration, yielding

$$\theta = 2 . \tag{4.4-4}$$

By contrast, both the value of z as well as that of the scaling function f depend on the exponent γ of Eq. (4.4.1) via the relation (Kolb in Stanley and Ostrowsky, 1985)

$$z = [1 - \gamma - (d - 2) / D]^{-1} . \qquad (4.4\text{-}5)$$

- For $\gamma < \gamma_c$ the function f is a bell-shaped curve,

  $f(x) \propto x^2\, g(x)$ where $g(x) << 1$, if $x >> 1$ or $x << 1$ [and $n_s(t)$ is then of the form t^{-2z}].

- For $\gamma > \gamma_c$ the function f is a monotone curve,

  $f(x) << 1$, if $x >> 1$ (exponential cut of large sizes), and
  $f(x) \propto x^{\delta}$ if $x << 1$, and $n_s(t)$ is of the form $t^{-z\delta}\, s^{-2+\delta}$.

The exponent δ is called the crossover exponent. Simulations in d = 3 give a critical value $\gamma_c \cong -0.27$, and numerical values of z and δ, as a function of γ, as given in the table below.

Table VI: Influence of diffusion [Eq. (4.4-1)] on growth

γ	–3	–2	–1	–1/D	–1/2	0	1/2
z	0.33	0.45	0.85	1	1.3	3	≅100
$2 - \delta$	–	–	–	–	≅0	1.3	1.87

4.4.2 Reaction-limited cluster–cluster aggregation

This model was created (Kolb and Jullien, 1984; Brown and Ball, 1985) to study the case where the sticking probability tends to zero (due to the presence of a potential barrier to be crossed before irreversible sticking takes place, as in the case of weakly screened colloids). The corresponding model for particle–cluster aggregation is the Eden model. Here again steric constraints due to the space occupied by each cluster lead to a lower fractal dimension than that of the dense Eden cluster (see the table in Sec. 3.4.1). Furthermore, the cluster dispersion plays a crucial role in reaction-limited cluster–cluster aggregation.

Cluster dispersion

In exactly hierarchical processes, the probability distribution of the cluster sizes peaks at a single value which varies in time: $n_s(t) = \delta[s - s_0(t)]$. In practice, monodispersity, of which the hierarchical model is an idealization, corresponds rather to a bell-shaped distribution centered on the mean cluster size. By

contrast, in a polydisperse system, all sizes are present but with a predominance of small clusters (with the n_s distributed as s^{-a}).

In the case of reaction-limited cluster–cluster aggregation, monodisperse systems are less dense. The fractal dimensions found by numerical simulation (Kolb and Jullien, 1984) are:

$$D \cong 1.55 \quad (d = 2) \qquad \text{and} \quad D \cong 2.00 \quad (d = 3) \,. \tag{4.4-6}$$

By contrast, polydispersity makes aggregates denser (Brown and Ball, 1984), the fractal dimensions then being

$$D \cong 1.59 \quad (d = 2) \qquad \text{and} \quad D \cong 2.11 \quad (d = 3) \,. \tag{4.4-7}$$

These last values are in good agreement with the experimental results described earlier (e.g., the gold aggregates in Fig. 3.4.5).

The Smoluchowski equation

The mean variation of the cluster size may be investigated by means of a kinetic equation due to Smoluchowski, which is based on the aggregation speeds K_{ij} of clusters of different sizes i and j (making a cluster of size i + j). This may be written

$$\boxed{dn_s(t)/dt = \frac{1}{2}\sum_{i+j=s} K_{ij}\, n_i(t)\, n_j(t) - n_s(t)\sum_{i=1}^{\infty} K_{is}\, n_i(t)} \,. \tag{4.4-8}$$

Many studies have been conducted concerning the form of the solutions to this equation using various expressions for K_{ij} (Leyvraz 1984; Ernst, in Pietronero and Tossati 1986, p. 289; see also Vicsek's book 1989, and the article on aggregation by Jullien, 1986). This may also be generalized to the reversible case in which clusters once formed may split again into two clusters.

4.4.3 Ballistic cluster–cluster aggregation and other models

In this third type of cluster–cluster aggregation model, the clusters may move freely (or diffuse with a large mean free path compared to the cluster size). Aggregation may be purely hierarchical (the monodisperse case) or, instead, correspond to a polydisperse process. The fractal dimension does not appear to depend on the dispersity, and the values obtained (see Family and Landau, 1984) are

$$D \cong 1.55 \quad (d = 2) \qquad \text{and} \quad D \cong 1.91 \quad (d = 3) \,. \tag{4.4-9}$$

These values are in agreement with measurements made on aerosols in a vacuum.

High density case

All the previous work has concerned situations in which the particle density is low. When this is the case, the clusters may effectively be considered as being situated on average reasonably far apart from one another. Highly dense systems behave differently. To try to understand the effect of high densities, in 1987, Kolb and Herrmann carried out a numerical study on a model in which the particle concentration was $\rho = 1$. The model was constructed as follows: all the lattice sites are initially occupied and bonds are created by making random attempts to displace the clusters already formed (starting with isolated particles) along vectors joining pairs of neighboring sites. Particles which enter into contact are then taken to be bonded, having returned to their initial positions.

In this model, surface or volume fractals are obtained depending on the value of γ. Thus, $\gamma = -2$ leads to surface fractals, $\gamma = 1$ to fractal aggregates, while when $\gamma = 2$ nonfractal objects are produced.

Reversible aggregation

All these modes of aggregation may be modified by allowing the possibility of reversible sticking of clusters or, more precisely, the possibility of clusters to divide in two. This type of process, which may also be investigated by means of Smoluchowski's equation, eventually leads to a steady state where the cluster size distribution is in equilibrium.

We shall not enter into further details concerning cluster–cluster aggregation as this is another very rich topic requiring a whole book to itself. Interested readers may consult the review articles relating to this subject or the book by Tamàs Vicsek dealing with growth phenomena (Vicsek, 1989 and 1991).